Hindawi Publishing Corporation
International Journal of Corrosion
Volume 2012, Article ID 451864, 5 pages
doi:10.1155/2012/451864

Research Article

Corrosion of Modified Concrete with Sugar Cane Bagasse Ash

R. E. Núñez-Jaquez,[1] J. E. Buelna-Rodríguez,[1] C. P. Barrios-Durstewitz,[1] C. Gaona-Tiburcio,[2] and F. Almeraya-Calderón[2,3]

[1] *Facultad de Ingeniería Los Mochis, Universidad Autónoma de Sinaloa, Fuente de Poseidón y Prol. Ángel Flores S/N, C.P. 87223 Los Mochis, SIN, Mexico*
[2] *Centro de Investigación e Innovación en Ingeniería Aeronáutica CIIIA, FIME-Universidad Autónoma de Nuevo León, Avenida Universidad S/N, Ciudad Universitaria, C.P. 87223 San Nicolás de los Garza, NL, Mexico*
[3] *Grupo Corrosión, Centro de Investigación en Materiales Avanzados, Miguel de Cervantes No. 120, C.P. 31109 Chihuahua, CHIH, Mexico*

Correspondence should be addressed to C. P. Barrios-Durstewitz, durstewitz.uas@gmail.com

Received 29 February 2012; Accepted 30 May 2012

Academic Editor: Andres A. Torres Acosta

Concrete is a porous material and the ingress of water, oxygen, and aggressive ions, such as chlorides, can cause the passive layer on reinforced steel to break down. Additives, such as fly ash, microsilica, rice husk ash, and cane sugar bagasse ash, have a size breakdown that allows the reduction of concrete pore size and, consequently, may reduce the corrosion process. The objective of this work is to determine the corrosion rate of steel in reinforced concrete by the addition of 20% sugar cane bagasse ash by weight of cement. Six prismatic specimens ($7 \times 7 \times 10$ cm) with an embedded steel rod were prepared. Three contained 20% sugar cane bagasse ash by weight of cement and the other three did not. All specimens were placed in a 3.5% NaCl solution and the corrosion rate was determined using polarization resistance. The results showed that reinforced concrete containing sugar cane bagasse ash has the lowest corrosion rates in comparison to reinforced concrete without the additive.

1. Introduction

Corrosion is the loss of material and occurs when metals are exposed to the environment. This is the result of the interaction between chemical and biological agents [1]. Corrosion of reinforced steel has two principal problems that affect the service life of concrete reinforced structures [2].

(a) Metal lost in the reinforced steel rods reduces the mechanical properties of the structure.

(b) Corrosion products occupy a higher volume than the base metal that produces internal stresses, which may cause the concrete to crack.

Degradation of concrete structures by corrosion processes is a serious problem and has major economic implications [3].

In service conditions, the concrete covering the steel bars gives physical and chemical protection to the reinforcement. The concrete cover provides an alkaline environment surrounding the steel, resulting in the formation of an oxide layer, called a passive film, which protects the steel from corrosion. However, the passive layer does not provide a perfect and permanent barrier in aggressive environments containing initiators of corrosion (primarily aggressive ions like sulphates and chlorides, humidity, carbon dioxide, and oxygen) [4]. These factors, together with inadequate construction practices in difficult environmental conditions, lead to corrosion of the reinforcing steel. Carbon dioxide can cause corrosion primarily by reducing the pH of the concrete. Once the alkaline environment is destroyed, the protective layer of oxide on the steel surface is destroyed and corrosion may start. Reinforced concrete structures are exposed to severe environments but often are expected to continue with little or no repair or maintenance for long periods of time. Therefore, reinforced concrete structures need to be durable. One of the main forms of attack from the environment is the ingress of chloride ions, which leads to corrosion of steel

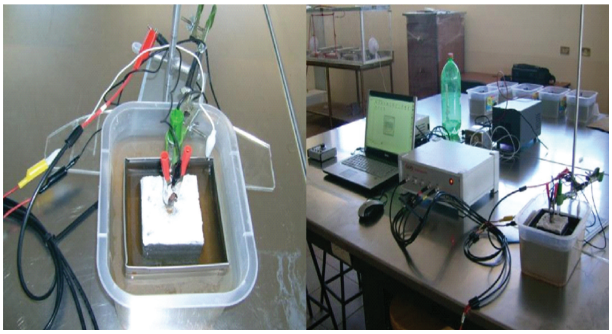

Figure 1: Experimental setup.

reinforcement and subsequent reduction in the resistance, utility, and esthetics of the structure [5]. Chlorides can come from several sources. They can be introduced into concrete during batching or can be introduced from the environment during service. Chlorides can be introduced by [6]

(a) the deliberate addition of chlorides in additives and use of seawater or contaminated aggregates in the mixture,

(b) saline mist and seawater, which moistens directly,

(c) deicing salts.

Mineral additives are commonly used in many applications ranging from high performance concrete bridges, buildings and on-shore and off-shore structures. Well-known mineral additives are silica fume, rice husk ash, and fly ash. The addition of these products in the production of concrete has positive environmental effects, while minimizing problems associated with its disposal [7].

Sugar cane bagasse is the by-product of sugar production. Fresh bagasse contains 40% water and often is used as fuel in the sugar factories. Sugar cane fiber has a particular significance because it is a combustible material for the sugar industry and is a valuable raw material for paper, artificial wood, and others [8]. When this waste is burned in controlled conditions, the generated ash contains amorphous silica, which has pozzolanic properties [9]. Ash from bagasse sugar cane is one of the main waste products generated worldwide and can be used as a mineral additive, mainly due to its high content of silica (SiO_2). Adding sugar cane bagasse ash (SCBA) as a replacement for cement may provide additional enhancements in resistance to chloride ion penetration and waterproofing properties. Thus, tests were conducted to determine whether SCBA can be used as an effective mineral additive for concrete reinforced structures [10].

2. Experimental Procedure

2.1. Materials. The materials used were portland cement (CPC-30R), river sand with a fineness modulus of 2.59, triturate river coarse aggregate with a maximum size of 3/4′′, and water. The sugar cane bagasse ash (SCBA) used in the present study was obtained from a local sugar factory in Los Mochis, Sinaloa, México. The ash was obtained from burning the bagasse at 650°C for one hour.

2.2. Thermogravimetric Analysis (TGA). The burn temperature of cane sugar bagasse required to obtain ash with amorphous SiO_2 was determined using TGA. The equipment employed was TA Instruments SIMULTANEOUS DTA-TGA STD 2.960 with a temperature scan rate of 10°C/min in a static atmosphere.

2.3. X-Ray Diffraction. After burning the bagasse, the ash was powdered and examined in an X-ray PANalytical Mod. X'Pert Pro.

2.4. Concrete Specimens. Four prismatic concrete specimens with dimensions of $100 \times 70 \times 70$ mm were constructed with a single 12 cm long 1018 steel rebar (0.9525 mm diameter) embedded in the concrete. In order to confine the exposed area of the steel, the rebar was partially coated with a noncorrosive paint, leaving an exposed length of 5 cm. The concrete was made with water to cement ratio of 0.60. Two specimens were made by replacing 20% by weight of the cement with sugar cane bagasse ash, and the remaining did not contain sugar cane bagasse ash. The specimens were cured by immersing in water for 28 days. After the curing period, the specimens were exposed to a solution of 3.5% by weight of sodium chloride.

Three 100 mm diameter by 200 mm long concrete cylinders with and without the addition of 20% bagasse cane ash were cast for the compressive strength tests.

In order to accelerate chloride ingress, the specimens were cyclically exposed to the sodium chloride solution by a 3-day partial immersion in a 3.5% weight NaCl solution followed by 4 days of drying.

2.5. Linear Polarization Resistance. The linear polarization resistance was determined with an ACM Instruments one-channel galvanostat/potentiostat GILL A.C. A standard calomel electrode (SCE) was used as the reference electrode, the rebar was the working electrode, and a stainless steel plate placed around the specimen was the counter electrode (Figure 1).

Table 1: Corrosion probability.

E_{corr} versus SCE (mV)	Corrosion probability
>−125	10% probability
−125 to −275	Uncertain zone
<−275	90% probability

Table 2: I_{corr} in terms of corrosion level.

I_{corr} (μA/cm^2)	Corrosion level
<0.1	Negligible
0.1–0.5	Low
0.5–1	Moderate
>1	High

The sweep potential was ±20 mV with respect to the corrosion potential and the sweep rate was 10 mV/minute. The IR drop potential was considered. This monitoring was conducted weekly with specimens immersed in the sodium chloride solution. Figure 2 shows the experimental setup. The results were analyzed using "Analysis" of ACM version 4 [11].

The corrosion current density (I_{corr}) and corrosion rate (CR) were estimated from resistance to charge transference (R_{ct}) using:

$$\text{Corrosion Current Density}\,(I_{corr}) = \frac{B}{R_{ct}}\,(\mu\text{A/cm}^2), \quad (1)$$

$$\text{Corrosion rate (CR)} = I_{corr}\,(\mu\text{A/cm}^2) * 0.011\,[=]\,\text{mmpy}, \quad (2)$$

where B is Stern-Geary constant (B = 26 mV for uniform corrosion) [12].

There are several techniques to determine the degree of deterioration of concrete structures. One is to determine the corrosion potential (E_{corr}) in accordance with ASTM-C-876, which establishes criteria that relate the potential with corrosion probability, as shown in Table 1 [13].

From the corrosion current density values (I_{corr}), obtained using (1), it is possible to determine the corrosion severity using the values shown in Table 2 [14].

3. Results and Discussion

Figure 2 shows the results of the thermogravimetric analysis (TGA). The thermograph shows that around 550°C there is no further decrease in weight. At this temperature, all of the sugar cane bagasse completely burned, but this is with a small sample of bagasse cane. With a greater amount of bagasse ash, it was necessary to burn at a higher temperature. For this reason, the sugar cane bagasse was burned at 650°C for one hour to obtain the ash for this study.

Figure 3 shows the X-ray powder diffraction pattern of SCBA burned at 650°C. The characteristic wide hump (between 2θ = 20 and 2θ = 35) and the peak of quartz show the presence of an amorphous phase, which is important to confirm because amorphous SiO_2 contributes to the pozzolanic properties. The ash pozzolanic reaction decreases the pore size in the concrete, which restricts entry of aggressive ions.

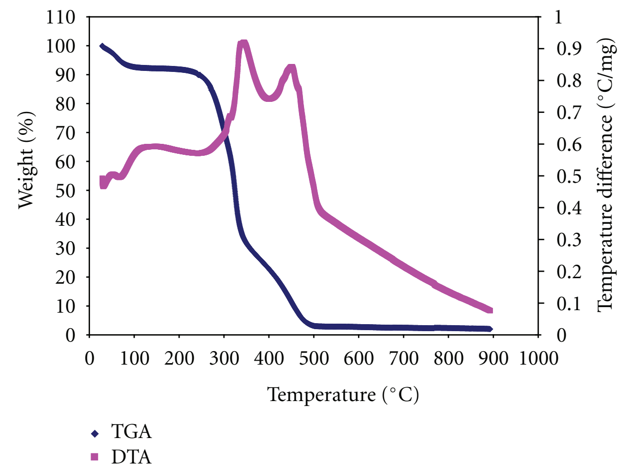

Figure 2: Thermograph of sugar cane bagasse.

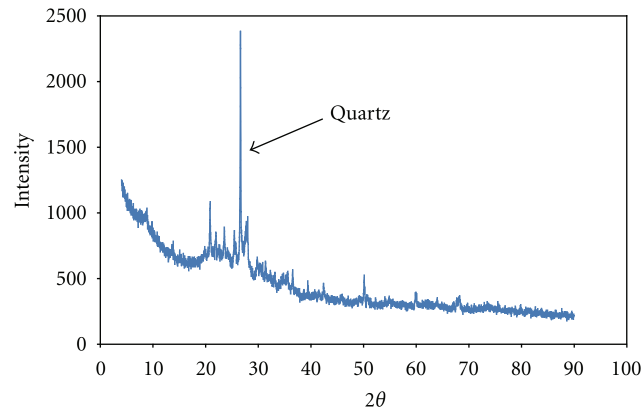

Figure 3: X-ray diffractogram of SCBA burned at 650°C.

Figure 4 shows the corrosion potential (E_{corr}) results obtained from linear polarization resistance scans of the six specimens. The corrosion potentials ranged between −100 and −550 mV. The specimens with SCBA (Bagasse 1 and 2) present smaller probability of corrosion compared with specimens without the additive (Normal 1 and 2). The horizontal dotted line represents the limit between regions of probability of corrosion as given in Table 1. During the first 15 days of exposure, the values are in the uncertain zone. Gradually, the normal concretes (without SCBA additive) became more negative to values in the 90% of corrosion probability. However, the concretes with SCBA continued in the uncertain zone, in the uncertain zone, after 63 days of cyclical exposure a great difference in the corrosion potential is observed between the specimens with and without SCBA. The normal concrete specimens have started to corrode.0020The specimens with SCBA show the smaller corrosion potential, which is probably due to SCBA reacting with calcium hydroxide (produced during the hydration of portland cement), and thenhydrated compounds formed

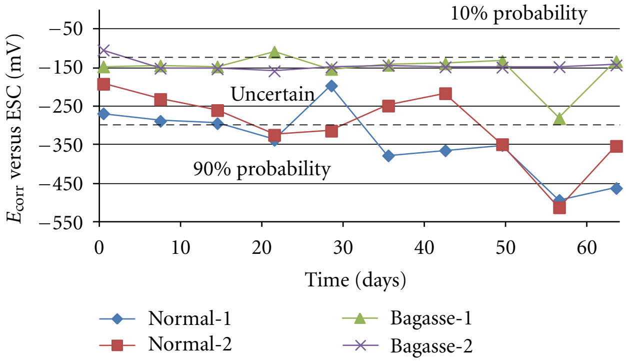

Figure 4: Corrosion potential of specimens.

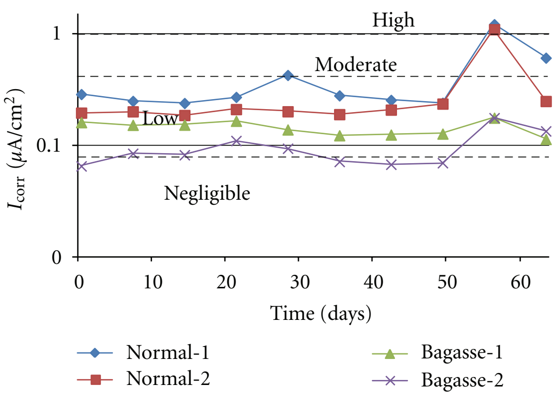

Figure 5: Corrosion current density of specimens.

during the pozzolanic reactions fills the pores of the concrete [15], restricting aggressive ions from reaching the steel rebar.

Figure 5 shows the corrosion current density (I_{corr}) results. I_{corr} ranged between 0.1 and 1.0 μA/cm^2. During the first 50 days, I_{corr} were from less than 0.1 μA/cm^2 for the concrete with SCBA. According to Table 2, the corrosion level is negligible. For normal concretes (without SCBA), I_{corr} values ranged between 0.1 μA/cm^2 and 0.5 μA/cm^2 for the first 50 days indicating that corrosion was low. However, after 50 days, I_{corr} gradually increased for the specimens without SCBA and is in the high corrosion level but the concrete with SCBA is still in the low corrosion level.

Figure 6 shows the corrosion rate results. At the beginning of the exposure, both types of specimens had similar results, but after day 50, the corrosion rate of the normal concrete without SCBA gradually increased. The specimens with SCBA showed lower corrosion rates. This behavior was due to the pozzolanic properties of SCBA that decreased the size of the concrete pores, which restricts the ingress of chloride ions.

4. Findings and Conclusions

(1) A temperature of 650°C was sufficient to obtain sugar cane bagasse ash with amorphous SiO_2.

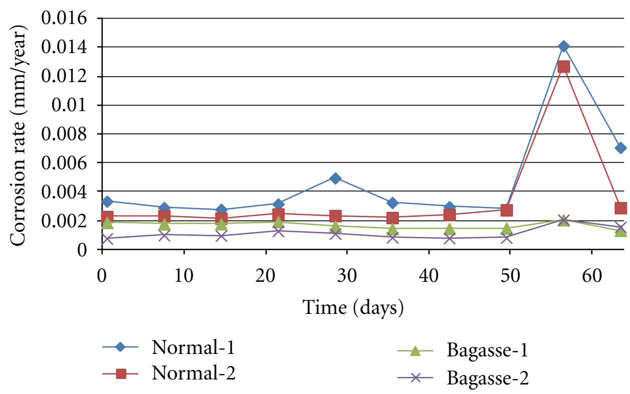

Figure 6: Corrosion rate of specimens.

(2) The specimens with SCBA indicated lower corrosion potential values, which corresponded to a low corrosion probability.

(3) The specimens with negligible to moderate corrosion level were the specimens with sugar cane bagasse ash added to the concrete mix.

(4) The use of sugar cane bagasse ash as a partial replacement of cement has a beneficial effect to protect the steel rebar from corrosion because it reduced the pore size in the cement paste, which minimized the ingress of aggressive ions into concrete. Concrete containing SCBA had a lower corrosion rate when compared to concrete without the addition of SCBA.

Acknowledgments

The authors express their gratitude to Ingenio Azucarero de Los Mochis for providing the sugar cane bagasse used in this investigation and also to Universidad Autónoma de Sinaloa, through Programa de Mejoramiento al Profesorado for the financial support of project PROMEP/103.5/08/3289, Folio UASPTC-022.

References

[1] A. Zaki, "Concrete corrosion: introduction to corrosion," in *Principles of Corrosion Engineering and Corrosion Control*, pp. 616–617, Butterworth-Heinemann, 2006.

[2] A. Del Valle, T. Pérez, and M. Martínez, "El Fenómeno de la Corrosión en Estructuras de Concreto Reforzado," Publicación técnica, Secretaría de Comunicaciones. y Transportes Instituto Mexicano Del Transporte, 2001.

[3] O. Covarrubias and P. Rodríguez, "Propiedades de Resistencia a la Corrosión de Aceros Aleados al Si Embebidos en Mortero," Ciencia UANL, 2001.

[4] R. Solís, E. Moreno, and P. Castro, "Durabilidad en la Estructura de Concreto de Vivienda de Zona Costera," Ingeniería de Revista Académica, 2005.

[5] K. Chandramouli, P. Srinivasa Rao, N. Pannirselvam, T. S. Seshadri Sekhar, and P. Sravana, "Chloride penetration resistance studies on concretes modified with alkali resistant glass fibers," *American Journal of Applied Sciences*, vol. 7, no. 3, pp. 371–375, 2010.

[6] P. Broomfield, "Causes and mechanisms of corrosion in concrete," in *Corrosion of Steel in Concrete*, Taylor and Francis, London, UK, 2007.

[7] G. C. Cordeiro, R. D. Toledo Filho, L. M. Tavares, and E. M. R. Fairbairn, "Pozzolanic activity and filler effect of sugar cane bagasse ash in Portland cement and lime mortars," *Cement and Concrete Composites*, vol. 30, no. 5, pp. 410–418, 2008.

[8] J. Osorio, F. Varon, and J. Herrera, "Comportamiento Mecánico del Concreto Reforzado con Fibras de Bagazo de Caña de Azúcar," *Dyna*, no. 153, 2007.

[9] N. B. Singh, V. D. Singh, and S. Rai, "Hydration of bagasse ash-blended portland cement," *Cement and Concrete Research*, vol. 30, no. 9, pp. 1485–1488, 2000.

[10] K. Ganesan, K. Rajagopal, and K. Thangavel, "Evaluation of bagasse ash as supplementary cementitious material," *Cement and Concrete Composites*, vol. 29, no. 6, pp. 515–524, 2007.

[11] ASTM G 59–97, "Standard Test Method for Conducting Potentiodynamic Polarization Resistance Measurements," American Society for Testing and Materials, 1997.

[12] S. Feliú, J. A. González, and C. Andrade, "*Electrochemical Methods for On site Determinations of Corrosion Rates Rebars*," Techniques to Assess the Corrosion Activity of Steel Reinforced Concrete Structures, ASTM STP 1276. ASTM, 1996.

[13] ASTM-C-876-91, "Standard Test Method for Half Cell Potentials of Reinforcing Steel in Concrete," ASTM , USA, 1992.

[14] O. Trocónis de Rincón, A. Romero de Carruyo, C. Andrade, P. Helene, and I. Díaz, "Descripción de métodos de ensayos," in *Manual de Inspección, Evaluación y Diagnostico de Corrosión en Estructuras de Hormigón Armado*, 1985.

[15] M. Frías, E. Villar-Cociña, and E. Valencia-Morales, "Characterisation of sugar cane straw waste as pozzolanic material for construction: calcining temperature and kinetic parameters," *Waste Management*, vol. 27, no. 4, pp. 533–538, 2007.